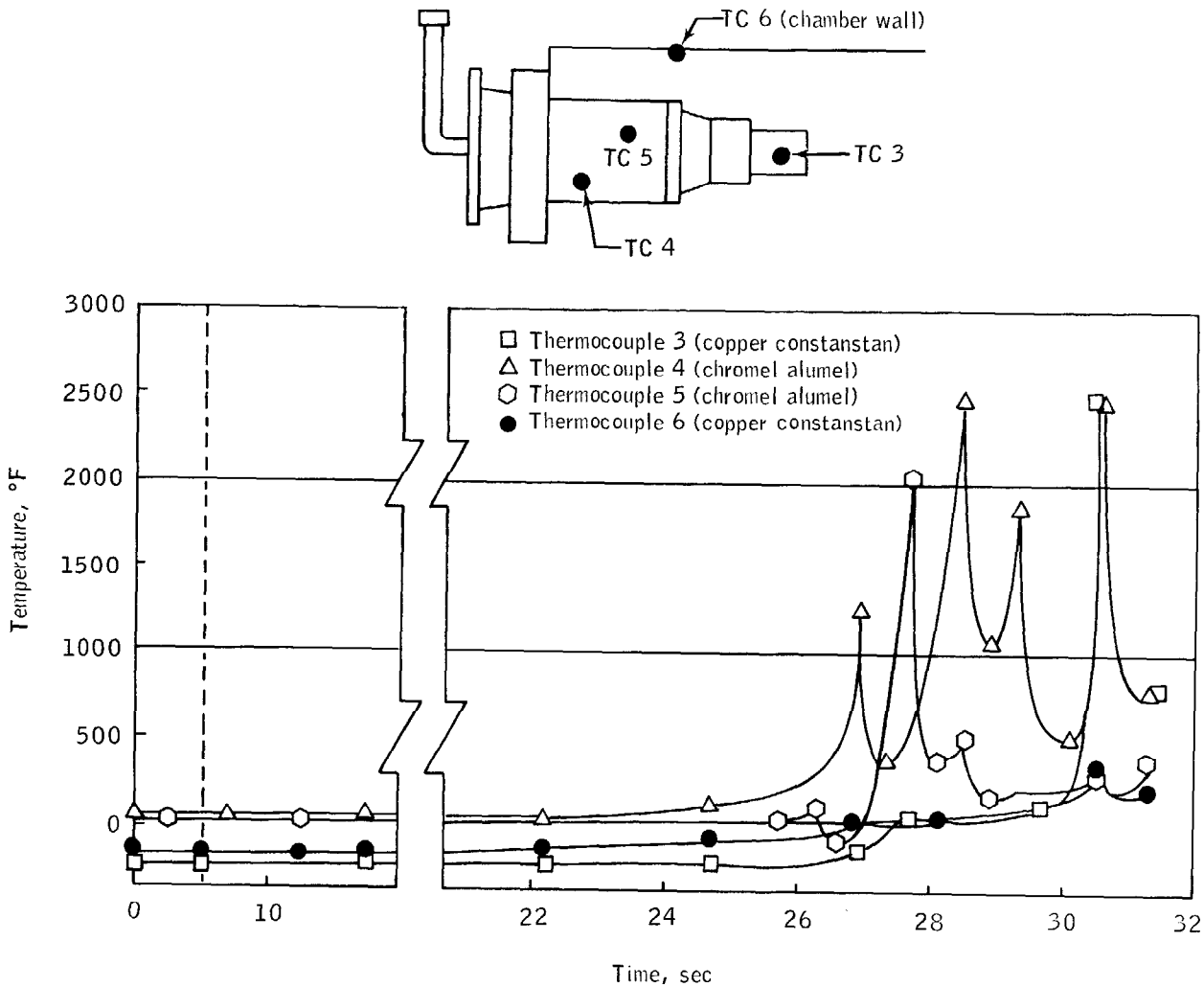

Figure F3.5-4.- Temperature history of quantity probe and chamber wall.

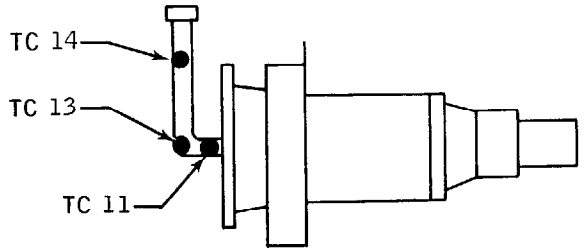

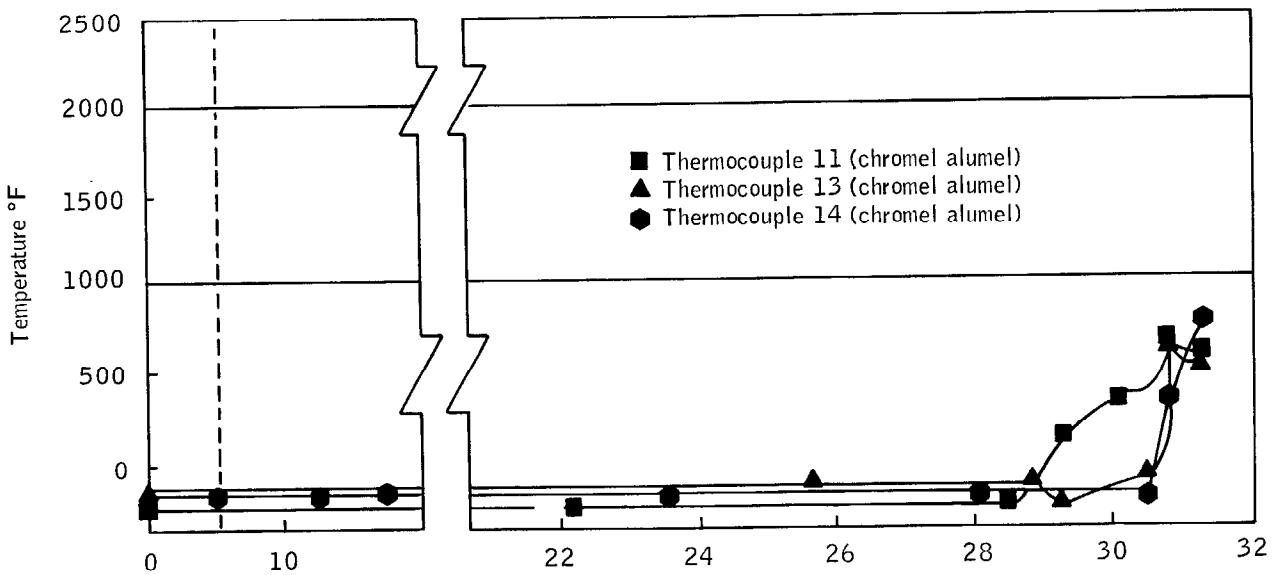

Figure F3.5-5.- Temperature history of conduit.

Figure F3.5-6.- Internal chamber view shortly after ignition.

Figure F3.5-7.- Burning along fan motor wire bundle.

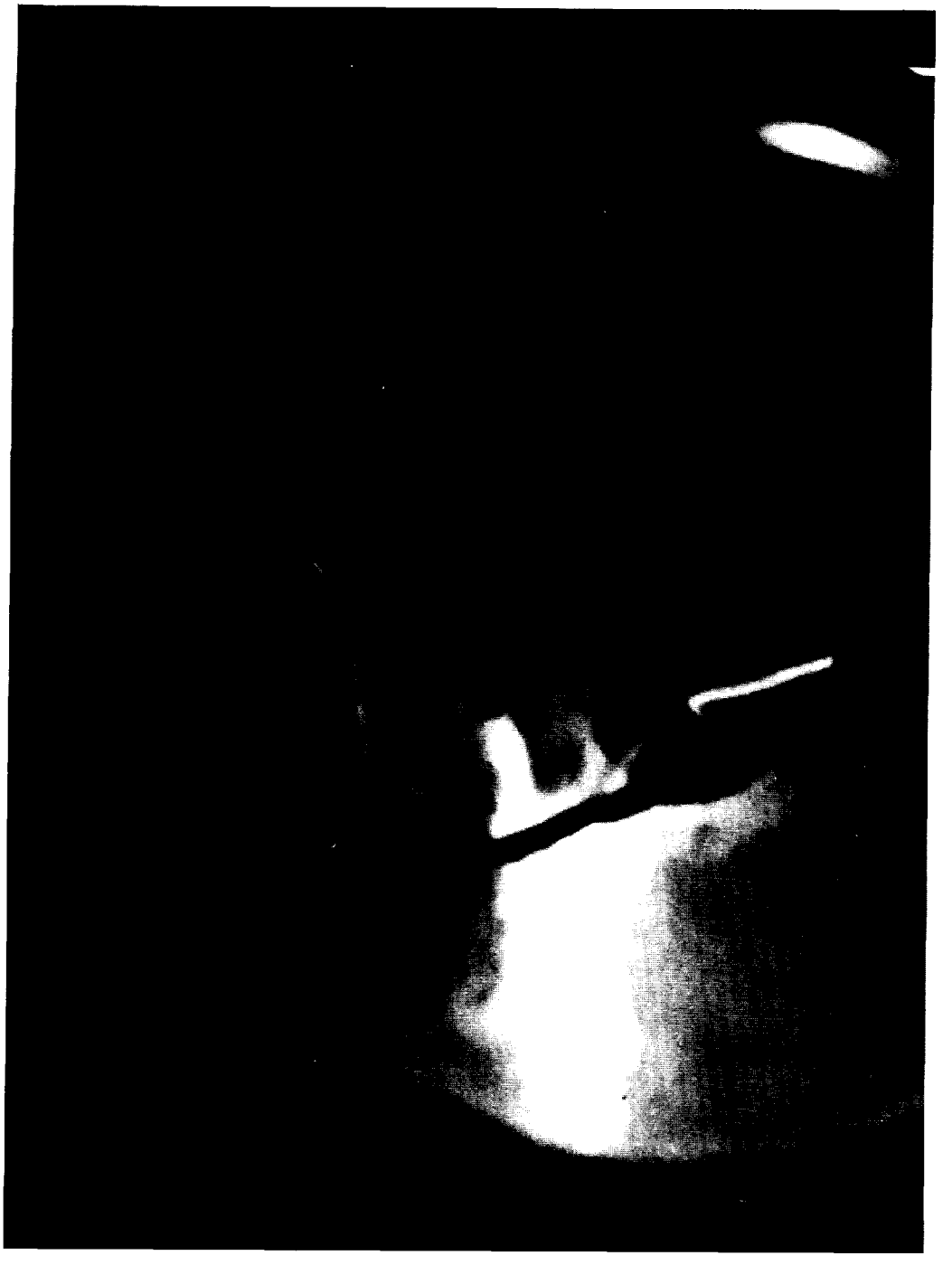

Figure F3.5-8.- Burning of adjacent wire bundles.

Figure F3.5-9.- Burning bundles prior to reaching probe insulator.

Figure F3.5-10.- Burning progressed into insulator.

Figure F3.5-11.- Dense smoke after propagation of burning into insulator.

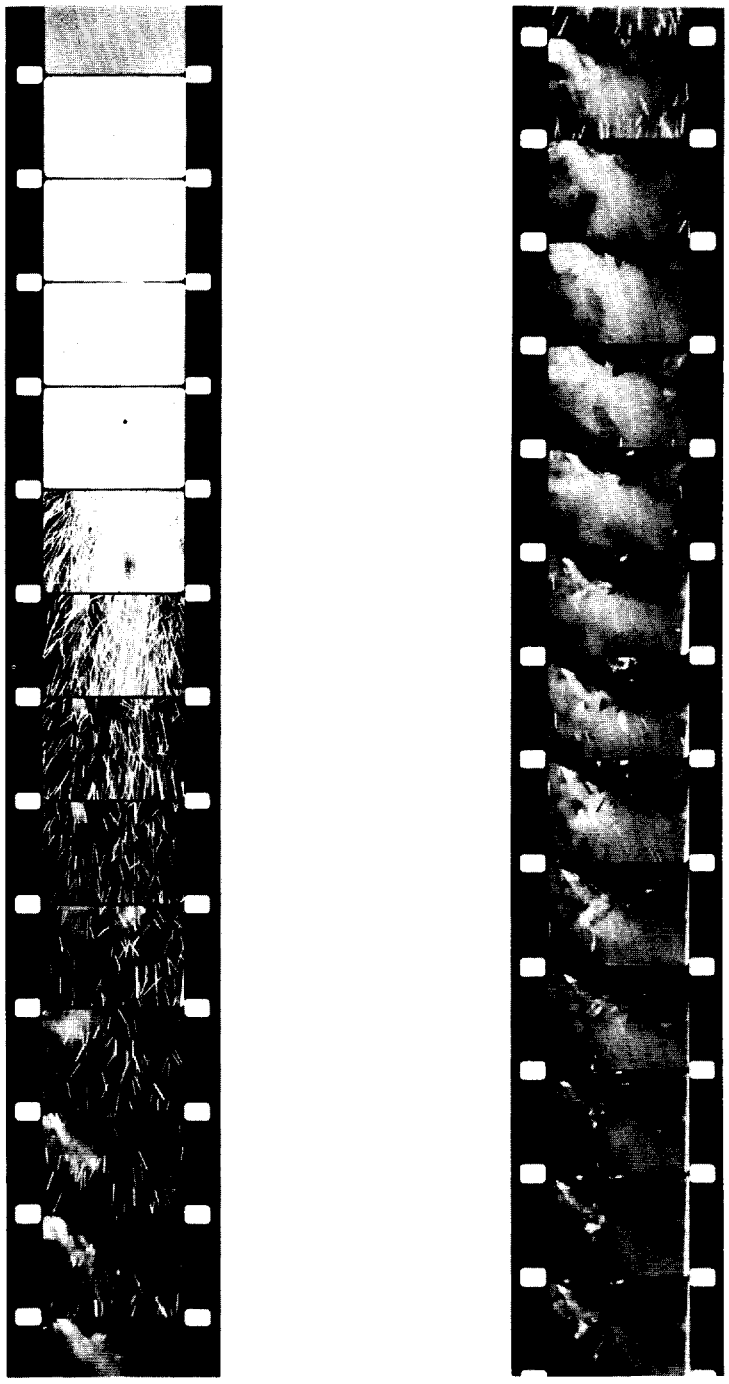

Figure F3.5-12.- External views of chamber-conduit interface at time of failure.

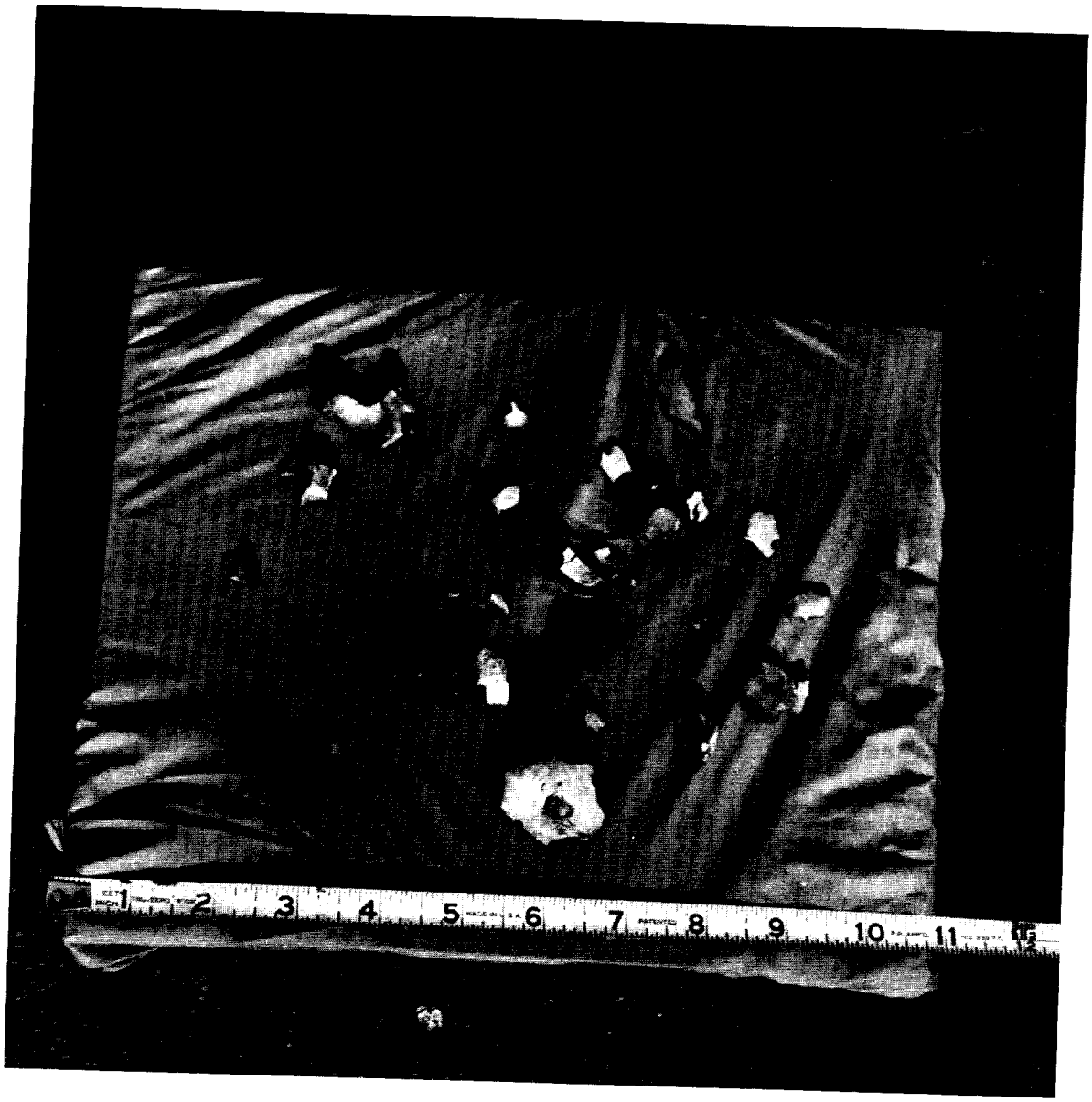

Figure F3.5-13.- Parts of probe insulator and tubing collected from area around test chamber.

Figure F3.5-14.- Portion of probe which remained in the test chamber.

Figure F3.5-15.- External view of chamber flange on which conduit-quantity probe interface was mounted (after test).

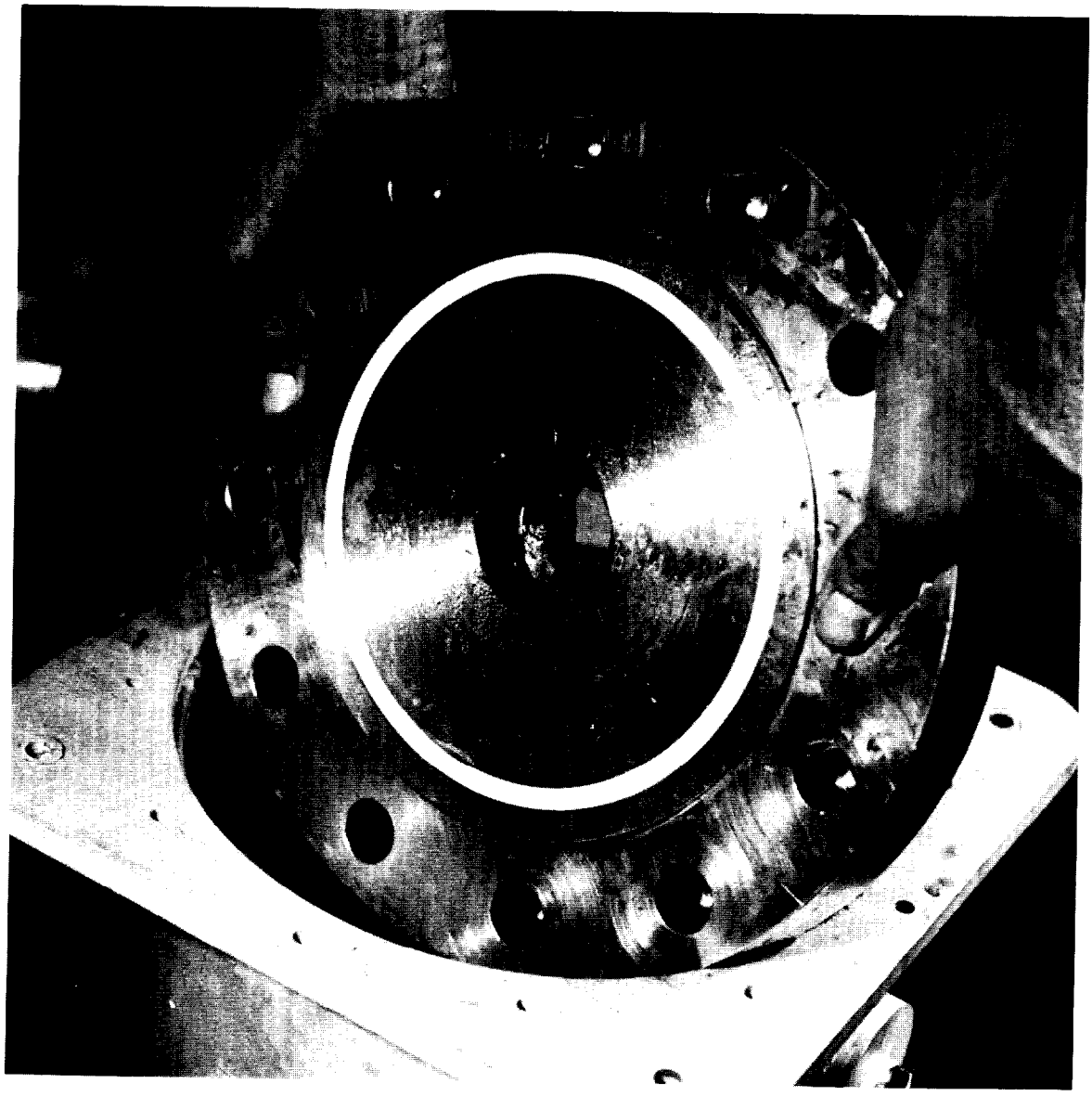

Figure F3.5-16.- View of chamber flange internal surface after test.

PART F3.6

ZERO-g TEFLON FLAME PROPAGATION TESTS

Objective

The objective of these tests was to measure the flame propagation rate along Teflon-insulated wire bundles in oxygen at 900 psia and -180° F in a zero-g environment. A second objective was to determine whether flames travelling along the fan motor lead wires would pass through the aperture in the motor case. Measurements are to be used to interpret the pressure and temperature history observed in the oxygen tank during the accident.

Apparatus

Tests were conducted at the Lewis Research Center's 5-Second Zero Gravity Facility. An experimental apparatus was designed and constructed which permitted the tests to be conducted in an oxygen environment of 920 psia ± 20 psi and -180° F ± 10°. The apparatus was installed on a standard drop test vehicle capable of providing the necessary supporting functions. An overall view of the drop vehicle is presented in figure F3.6-1 and a detailed photograph of the experimental apparatus is shown in figure F3.6-2. The basic components of the experimental apparatus are the combustion chamber with a sapphire window to permit high-speed photography, and an expansion tank as a safety feature in the event an excessive pressure rise were to occur. The apparatus was equipped with a fill and vent system, pressure relief system, and liquid nitrogen cooling coils. The test specimen was installed in the combustion chamber in a horizontal position as is shown in figure F3.6-3. This figure is typical of all installations. Ignition was caused by heating a 26-gage nichrome wire which was wrapped around the specimen. Chamber pressure and temperature were monitored throughout the test. High-speed photographic data (400 frames per second) were obtained using a register pin Milliken camera.

Approach

A total of eight tests were conducted on three test specimens. Each specimen was run in a one-g and a zero-g environment, and a one-g and zero-g test was repeated on two specimens to examine repeatability of the data. The three specimens were the following:

Type 1 - Fan motor conductor bundle - four wires and white sleeving

Type 2 - Fan motor conductor bundle - four wires and clear shrink sleeving

Type 3 - Aluminum Teflon feed-through assembly - four wires and no sleeving

The aluminum plate thickness for the Type 3 tests equaled that of the fan motor case. This specimen was used to determine whether a flame burning along the lead wires would continue through the aperture in a simulated motor case, and whether the aluminum would ignite.

Results

The zero-g linear propagation rate for fan motor wires in white pigmented Teflon sleeving (Type 1) was measured as 0.12 in/sec, and for the same wires in clear Teflon sleeving (Type 2), the rates in two separate tests were 0.16 and 0.32 in/sec. The corresponding flame propagation rate at one-g for both types of wire bundles was 0.55 in/sec measured in three tests. These results are listed in table F3.6-I. The flame in both zero-g and one-g tests pulsed as it spread along the wire bundles with the flame markedly more vigorous in the one-g cases. In all cases the Teflon was completely burned with little visible residue.

The flame propagation tests through an aluminum plate (Type 3) showed that the flame did not appear to have propagated through the Teflon grommeted aperture under zero-g conditions, but did pass through at one-g. Unfortunately, the pictures of the flames under zero-g were not clear enough to be certain that the flame failed to propagate through the aperture. Because the zero-g period lasts for less than 5 seconds following ignition, it is possible that flame propagation through the aperture would have been observed if more time at zero-g were available. These results are also listed in table F3.6-I.

Conclusions

The flame propagation rate along Teflon insulation in zero-g is reduced by about a factor of two from that observed in one-g. The propagation rate along the fan motor lead bundle in zero-g is in the range of 0.12 to 0.32 in/sec. These flame propagation rates are of a magnitude which is consistent with the time required to account for the duration of the pressure rise in the spacecraft oxygen tank.

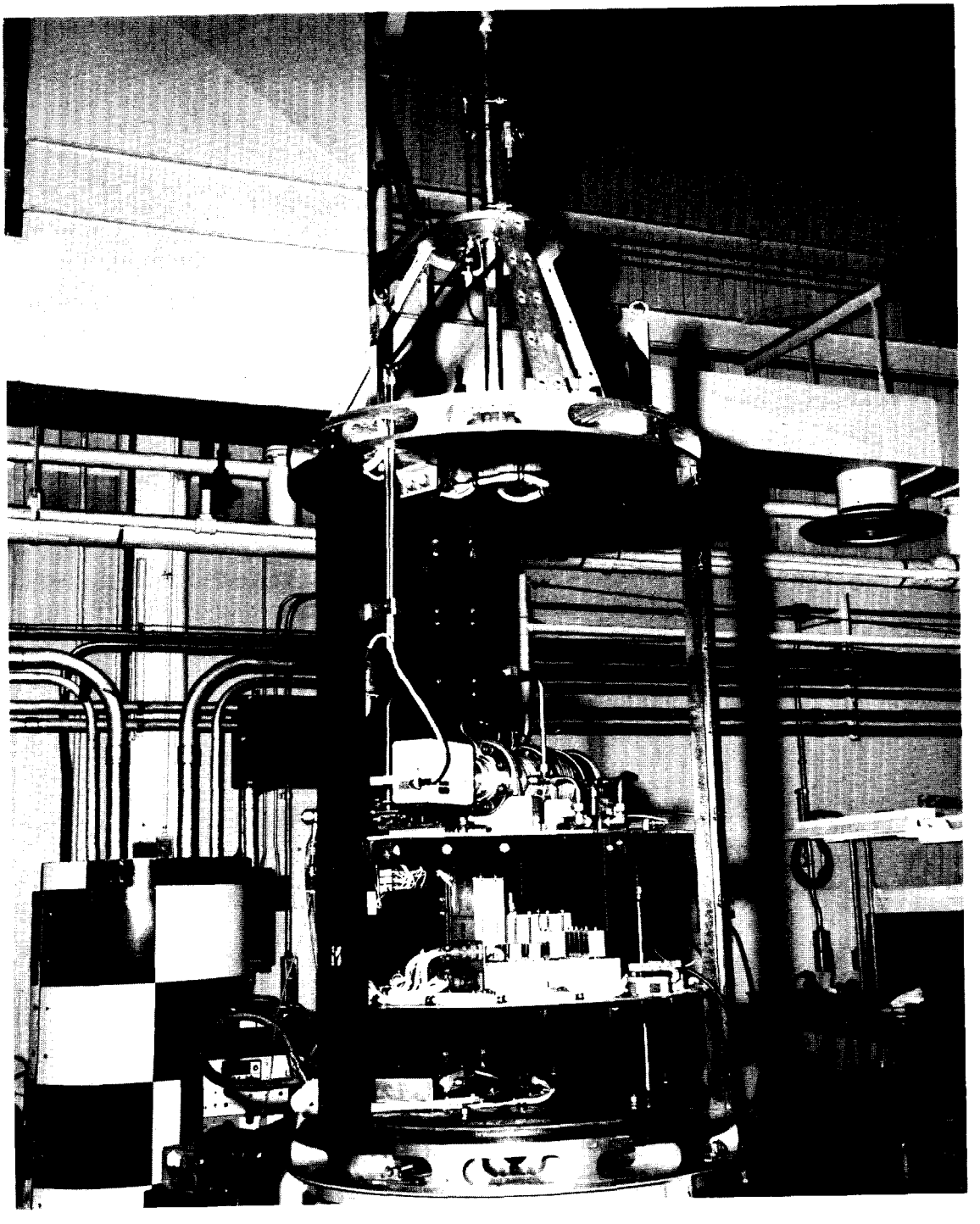

Figure F3.6-1.- 5-second drop vehicle.

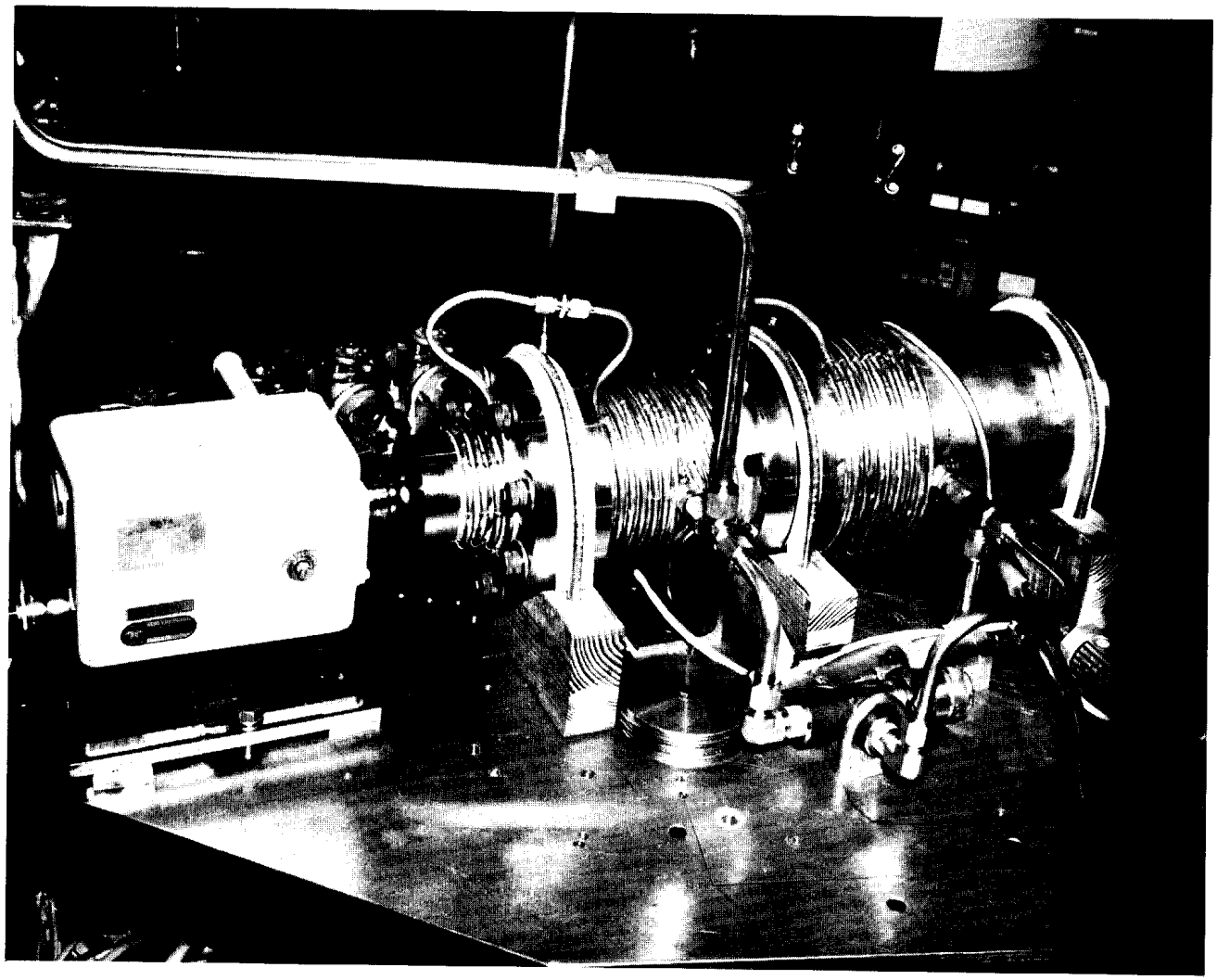

Figure F3.6-2.- Experimental combustion apparatus.

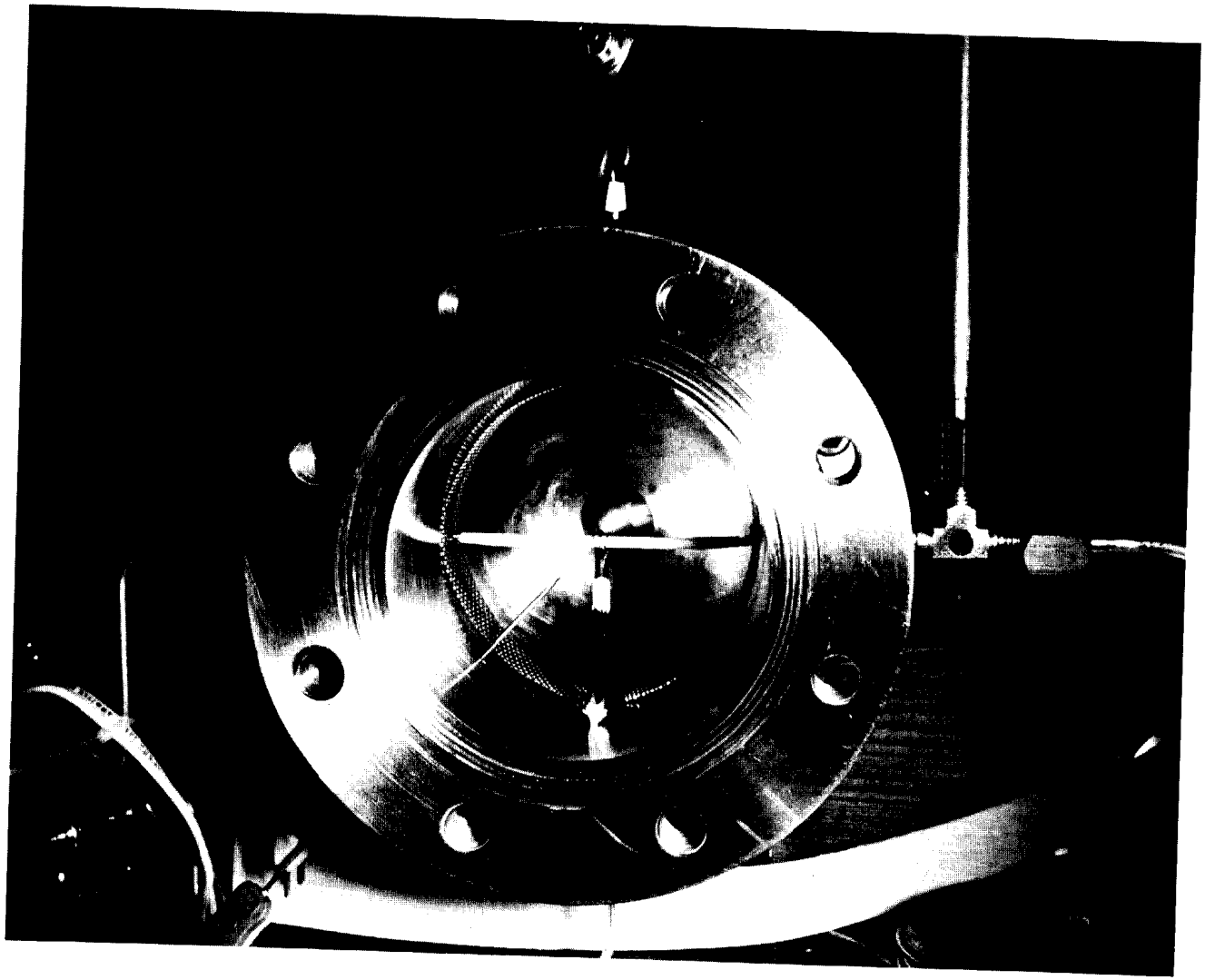

Figure F3.6-3.- Typical test specimen installation in combustion chamber.

TABLE F3.6-I.- SUMMARY OF RESULTS

Run no.	Test specimen	Gravity level	Average flame spread rate, in/sec	Comments
A-1-1 A-1-2 A-1-6	Type 1 Type 2 Type 1	One One One	0.55 0.55 0.55	The specimens burned vigorously. The flame progressed along the specimens in a pulsating fashion.
A-1-3 A-1-5 A-1-7	Type 2 Type 1 Type 2	Zero Zero Zero	0.16 0.12 0.32	The specimens burned in zero-g but not as vigorously as in normal gravity. The flame pulsated along the specimens in a similar way as in normal gravity but at a slower overall rate.
A-1-8	Type 3	One	-	The flame propagated through the aluminum holder but did not ignite it.
A-1-4	Type 3	Zero	-	The flame could not be clearly defined on the film. The aluminum holder did not ignite.

PART F3.7

FULL-SCALE SIMULATED OXYGEN TANK FIRE

Objectives

The purpose of this test was to simulate as closely as possible, in a one-g environment, the processes that occurred during the failure of oxygen tank no. 2 of Apollo 13. The data to be obtained include the pressure and temperature history which results from the combustion of Teflon wire insulation beginning at one of three likely ignition locations, as well as observing the manner in which the tank or conduit fails and vents its contents.

Apparatus

A Block I oxygen tank was modified to Block II configuration. The vacuum dome was removed and the tank was mounted in a vacuum sphere with the appropriate size and length of tubing connected. The heaters were disconnected and three hot-wire ignitors were installed. One ignitor was located on the bottom fan motor leads, one on the top fan motor leads, and another on the wire loop between the quantity probe and the heater-fan support. The connecting tubing, filter, pressure transducer and switch, relief valve, and regulator were flight-qualified hardware. The tank was mounted so that the long axis of the quantity probe was horizontal. Figure F3.7-1 shows the tank mounted in the chamber. Two television cameras and four motion picture cameras were mounted in the vacuum chamber. One camera operates at 64 frames/sec, two at 250 frames/sec, and another at 400 frames/sec. The two 250 frames/sec cameras were operated in sequence.

Results

The nichrome wire ignitor on the bottom fan motor leads was ignited. The tank pressure rose from an initial value of 915 psia to 990 psia in 48 seconds after ignition. The temperature measured by the flight-type resistance thermometer, mounted on quantity gage, rose 3° F from an initial value of -202° to -199° F in this 48-second period. The tank pressure reached approximately 1200 psia at 56 seconds after ignition and apparently the flight pressure relief valve which was set to open at 1005 psia could not vent rapidly enough to check the tank pressure rise. Two GSE pressure relief valves, set at higher pressures, apparently helped to limit the tank pressure to 1200 psia. The tank temperature rose abruptly after 48 seconds, following ignition, from -199° to -170° F in 3 seconds. After this time the temperature read off-scale above

2000° F. Failure of the temperature measuring wiring is indicated by the erratic readings that followed. These data are shown in figure F3.7-2. The pressure data shown beyond 56 seconds represent the venting of the tank contents. These pressure and temperature histories are qualitatively similar to the measured flight data but occur more rapidly than observed in flight.

The conduit failed close to where it attaches to the tank closure plate about 57 seconds after ignition (fig. F3.7-3). The two 250-frame/sec cameras and the 64-frame/sec camera failed to operate during this test. However, the 400-frame/sec camera suggests that the first material to issue from the ruptured conduit was accompanied by bright flame. The tank pressure declined from 1175 psia to 725 psia in 1 second following conduit rupture. High oxygen flow rates were observed from the conduit breach for about 15 seconds. A posttest examination of the ruptured conduit showed that the expulsion of the tank contents was limited by the 1/2-inch-diameter aperture in the tank closure plate. An examination of the internal components of the tank showed complete combustion of the Teflon insulation on the motor lead wires as well as almost complete combustion of the glass-filled Teflon sleeve. This is shown in figure F3.7-4.

Conclusions

The qualitative features of the pressure and temperature rises in oxygen tank no. 2 have been simulated by initiating Teflon wire insulation combustion on the lower fan motor lead wire bundle. The time from ignition of the total combustion process in the simulated tank fire is about three-fourths to one-half the time realized in the spacecraft accident. The conduit housing the electrical leads failed near the weld and resulted in a limiting exit area from the tank of about 1/2 inch diameter. The venting history is characteristic of the expulsion of liquid for the first 1-1/2 seconds. This was followed by a two-phase flow process.

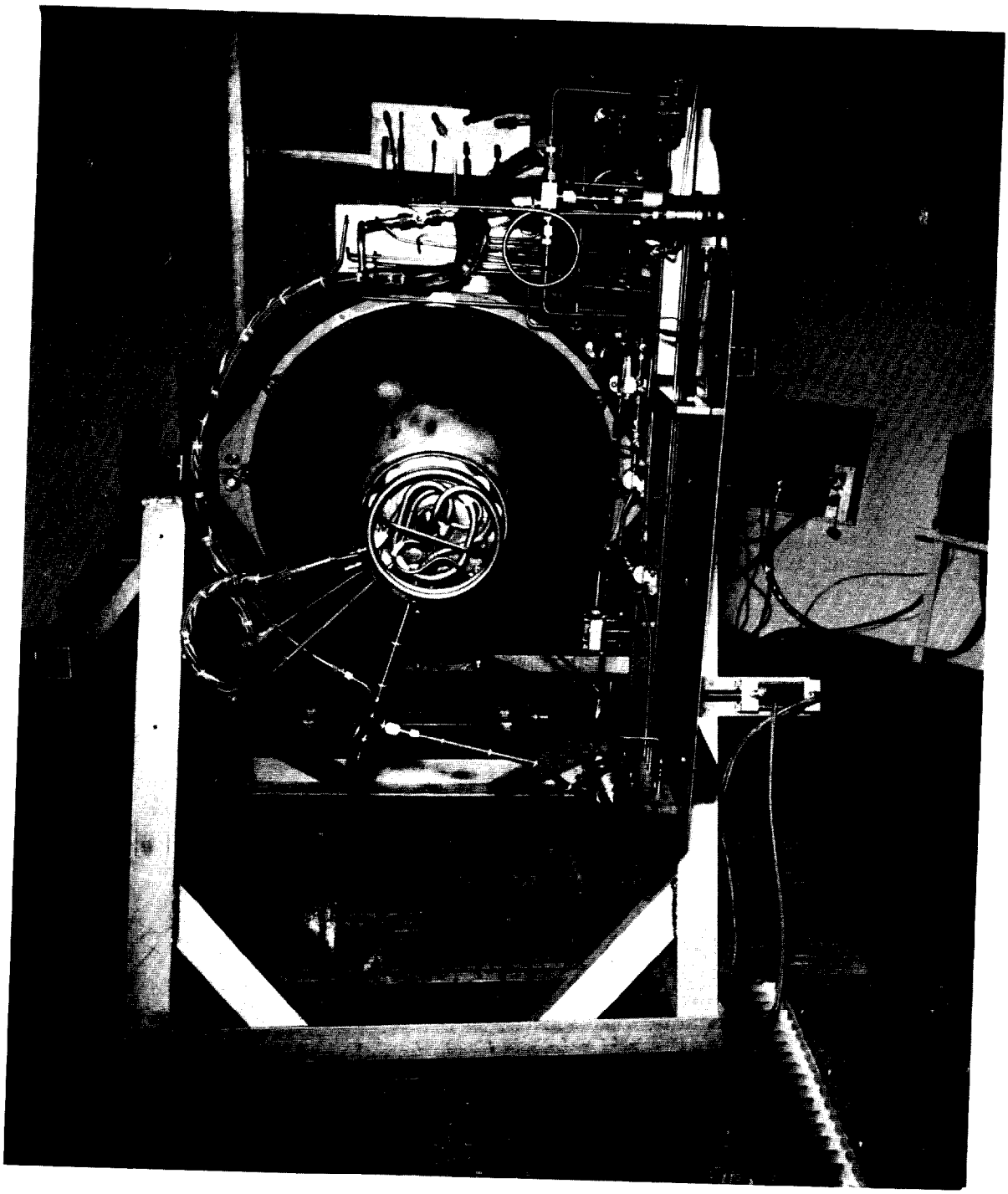

Figure F3.7-1.- Posttest oxygen tank setup.

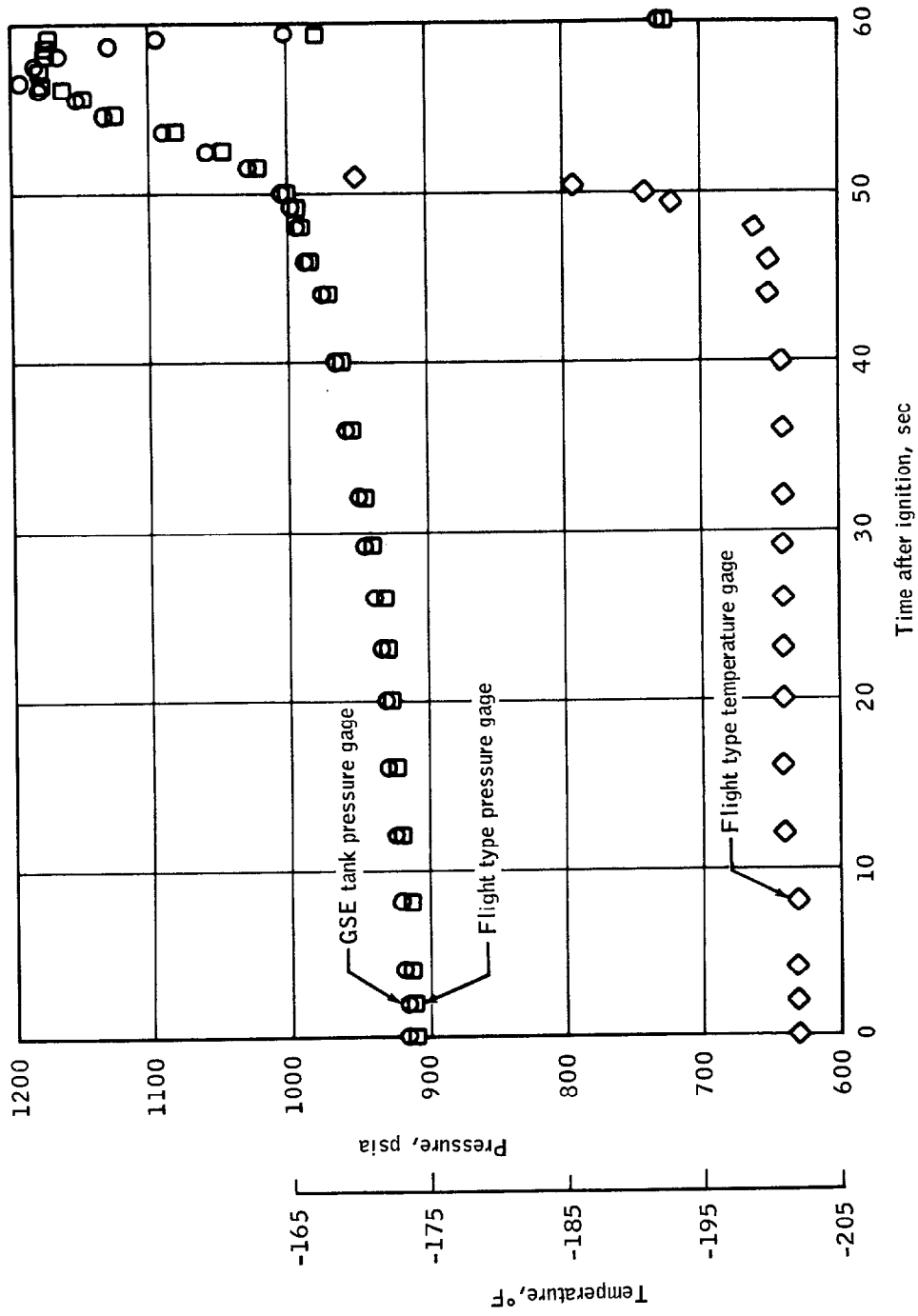

Figure F3.7-2.- Measured pressure and temperature time histories (preliminary data as of June 4, 1970).

(a) Wide-angle view.

Figure F3.7-3.- View of failed conduit.

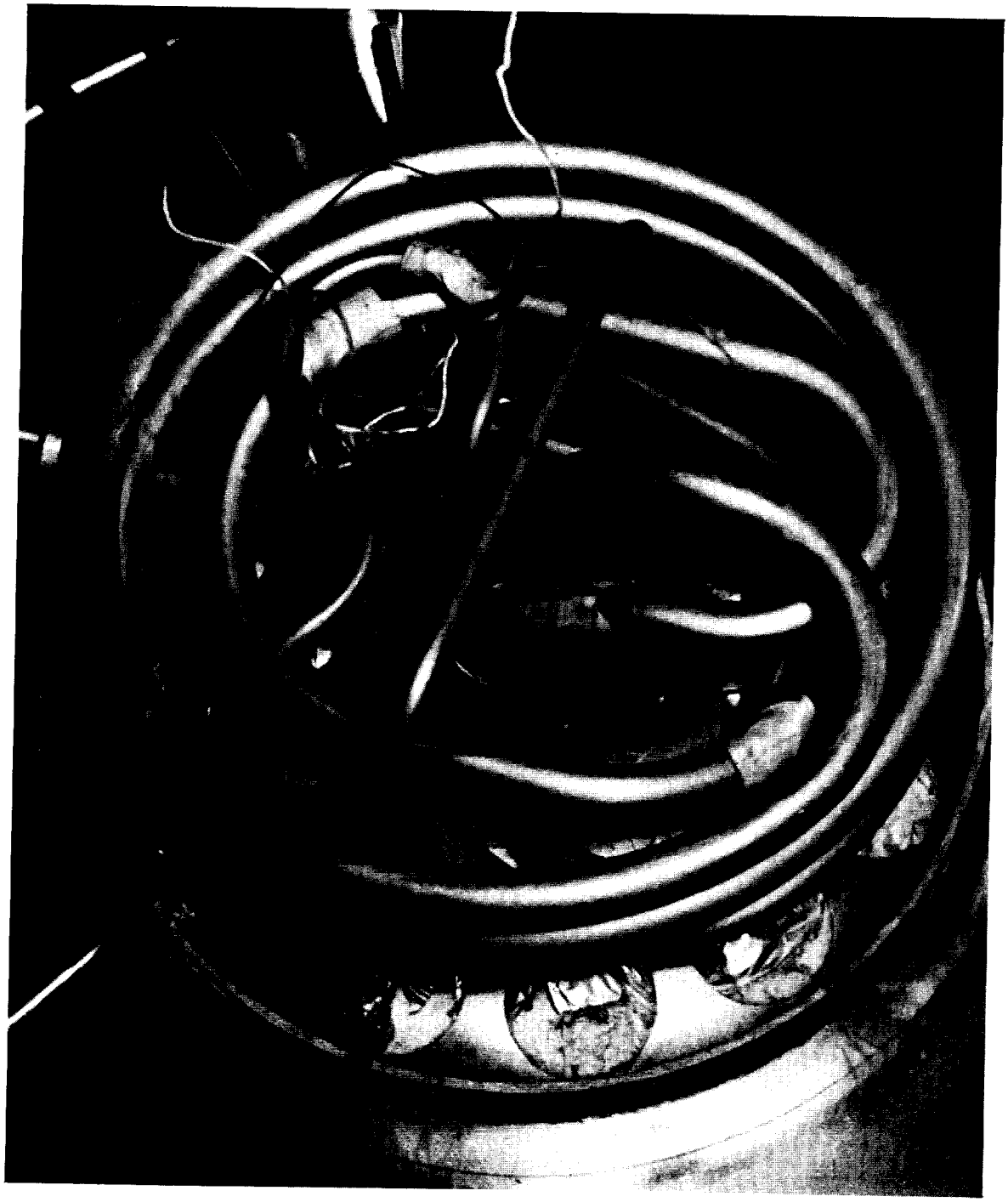

(b) Closeup view.

Figure F3.7-3.- Concluded.

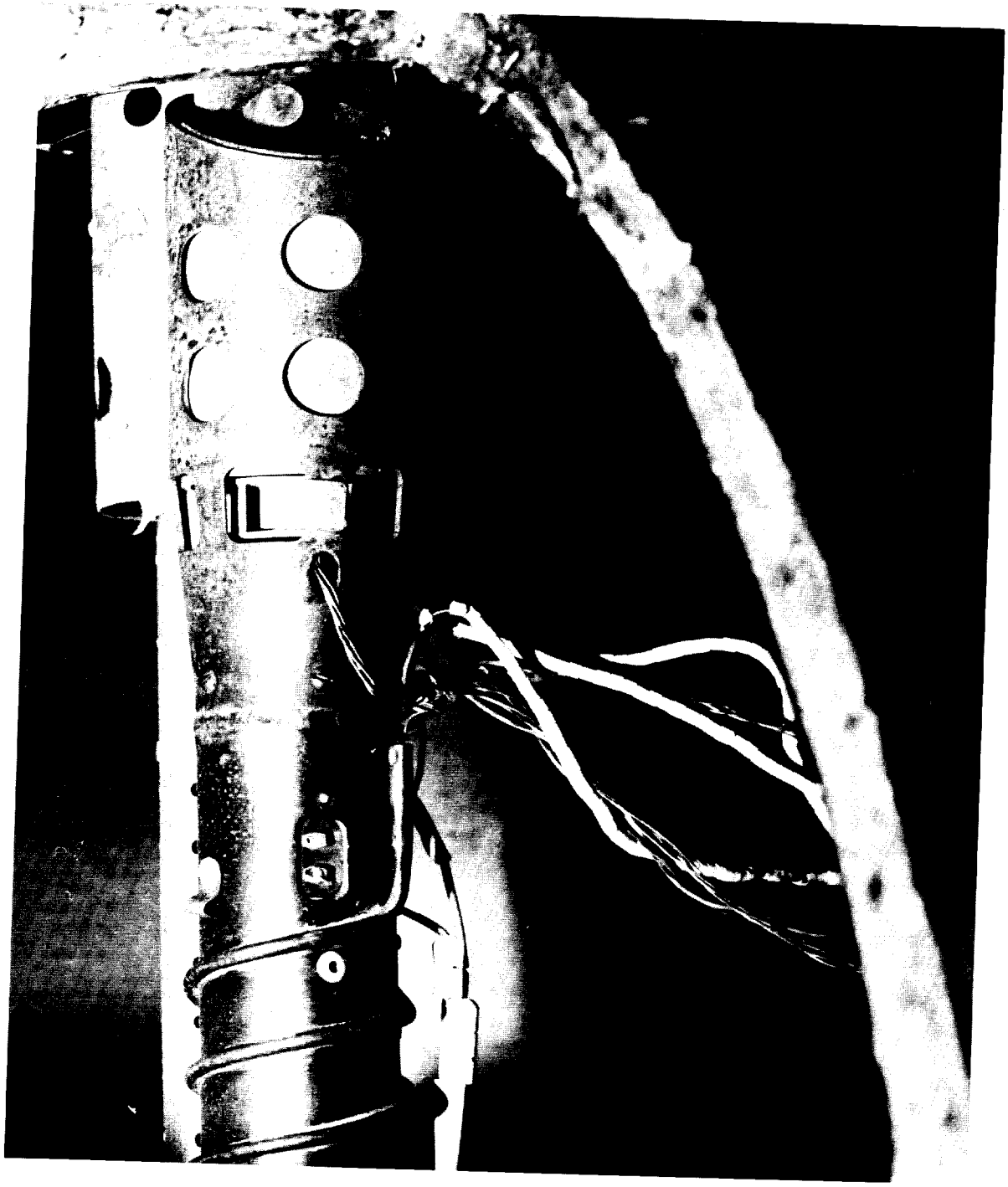

Figure F3.7-4.- Posttest internal view of tank components.

PART F3.8

ANALYSIS OF FLOW FROM RUPTURED OXYGEN TANK

Objective

The objective of this analysis was to compute the real gas discharge rate from the cryogenic oxygen tank no. 2 and provide the subsequent pressure history of various service module volumes.

Assumptions

1. Oxygen remains in equilibrium at all times. The oxygen properties were obtained from the tabulations and plots of references 2 and 3.

2. All orifice coefficients were taken to be unity and the orifices assumed to be choked.

3. All volumes and areas are invariant with time.

4. The effective volume of the oxygen tank is 4.7 ft^3 and is not changed by combustion processes.

5. All processes are isentropic both inside the oxygen tank and also between the oxygen tank and its discharge orifice.

6. Oxygen thermodynamic properties (ρ, p, h) are uniform throughout any given individual volume at any time.

7. The processes in volumes external to the oxygen tank are adiabatic. The total enthalpy in these volumes is equal to the average enthalpy of all prior discharged oxygen. Each volume acts as a plenum chamber for its respective vent orifice.

8. The initial tank conditions at t = 0 are p = 900 psi; ρ = 47.4 lb/ft^3; T = -190° F.

Method

Computations were based on several manually generated cross plots of the thermodynamic properties, correlations of intermediate computed results; and analytical and numerical integrations involving these

correlations. Choked orifice states were obtained by maximizing ρu for a given entropy.

Results

Figure F3.8-1 shows the mass flow rate per unit of effective orifice area plotted as a function of time. The two time scales shown are applicable to effective orifice diameters of 0.5 inch and 2.0 inches.

Figure F3.8-2 plots the total mass discharged from the oxygen tank against the same two time scales.

Figures F3.8-3 and F3.8-4 are plots of pressure time histories for various combinations of secondary volumes and orifices. The time scale in this case is only applicable to the 2-inch diameter exit orifice in the oxygen tank. The combinations of V and A* shown in figure F3.8-3 were chosen to roughly simulate the components of the SM as follows:

1. $V = 25\ ft^3$, $A^* = 2.08\ ft^2$ ($300\ in^2$). Simulates net volume of the oxygen shelf in bay 4 with effective venting of $300\ in^2$.

2. $V = 67\ ft^3$, $A^* = 2.08\ ft^2$ ($300\ in^2$). Simulates the bay 4 oxygen shelf and fuel cell shelf combined volume with venting of $300\ in^2$.

3. $V = 67\ ft^3$, $A^* = 1.39\ ft^2$ ($200\ in^2$). Same as case 2 but reduced venting area to rest of service module.

4. $V = 100\ ft^3$, $A^* = .43\ ft^2$ ($62\text{-}1/2\ in^2$). Simulates entire bay 4 with small venting.

5. $V = 200\ ft^3$, $A^* = .43\ ft^2$ ($62\text{-}1/2\ in^2$). Simulates combined bay 4 and tunnel volumes with venting past rocket nozzle only.

Also plotted are reference curves for each of the above volumes without any venting ($A^* = 0$).

Case 1 has a very rapid initial pressure rise with time due to the small volume ($25\ ft^3$) of the oxygen shelf. However, the mass efflux from this volume also increases rapidly with time so that it equals the influx at $t = 0.18$ second and the pressure peaks at approximately 8.8 psia.

---

*If the tank were initially at $p \approx 1000$ psi and the same entropy, then with a 2-inch diameter orifice the pressure would drop to 900 psi in 0.004 second with the discharge of 1 lb_m oxygen.

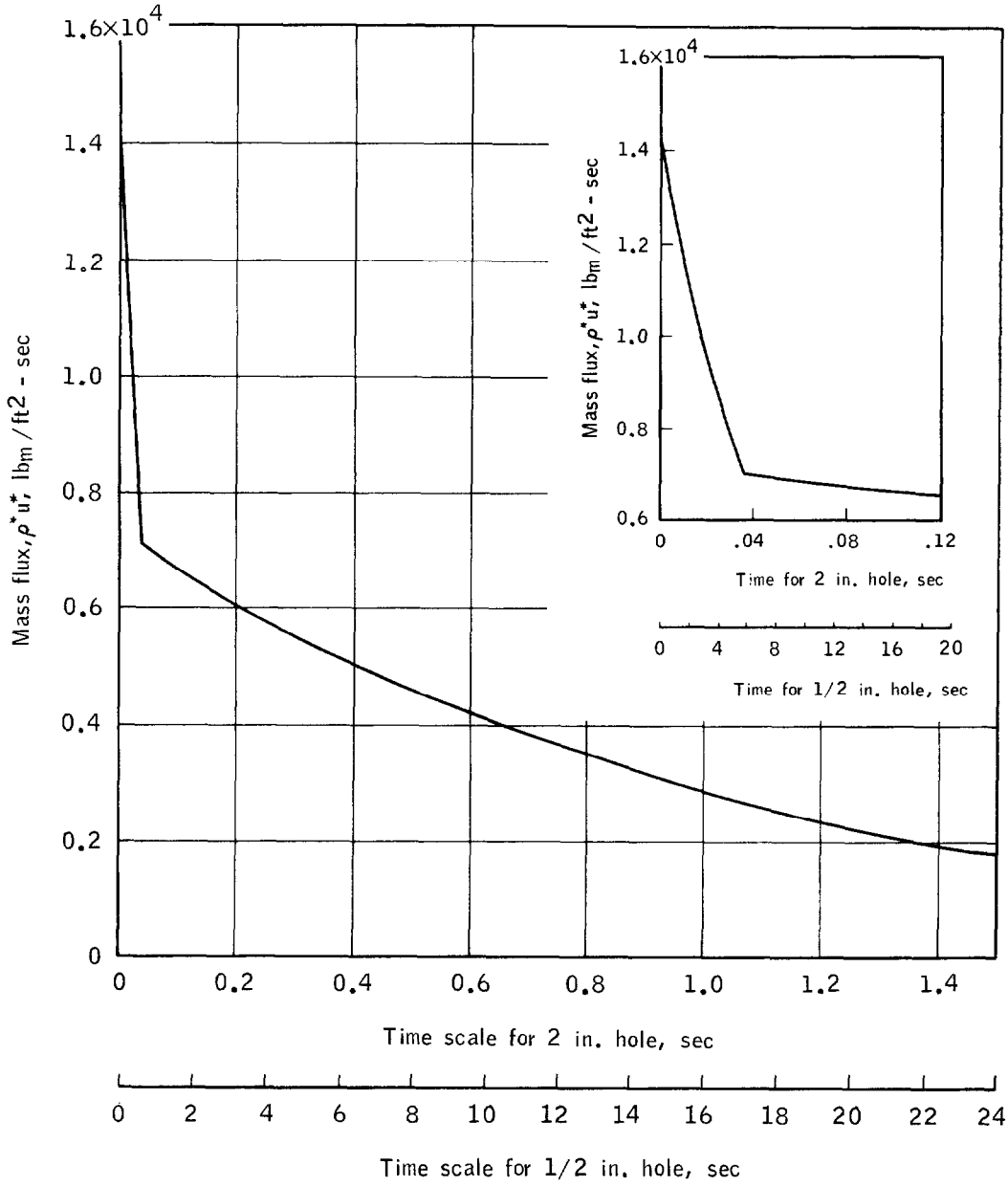

Figure F3.8-1.- Mass flow per unit area against time for 2 inch and 0.5 inch orifices.

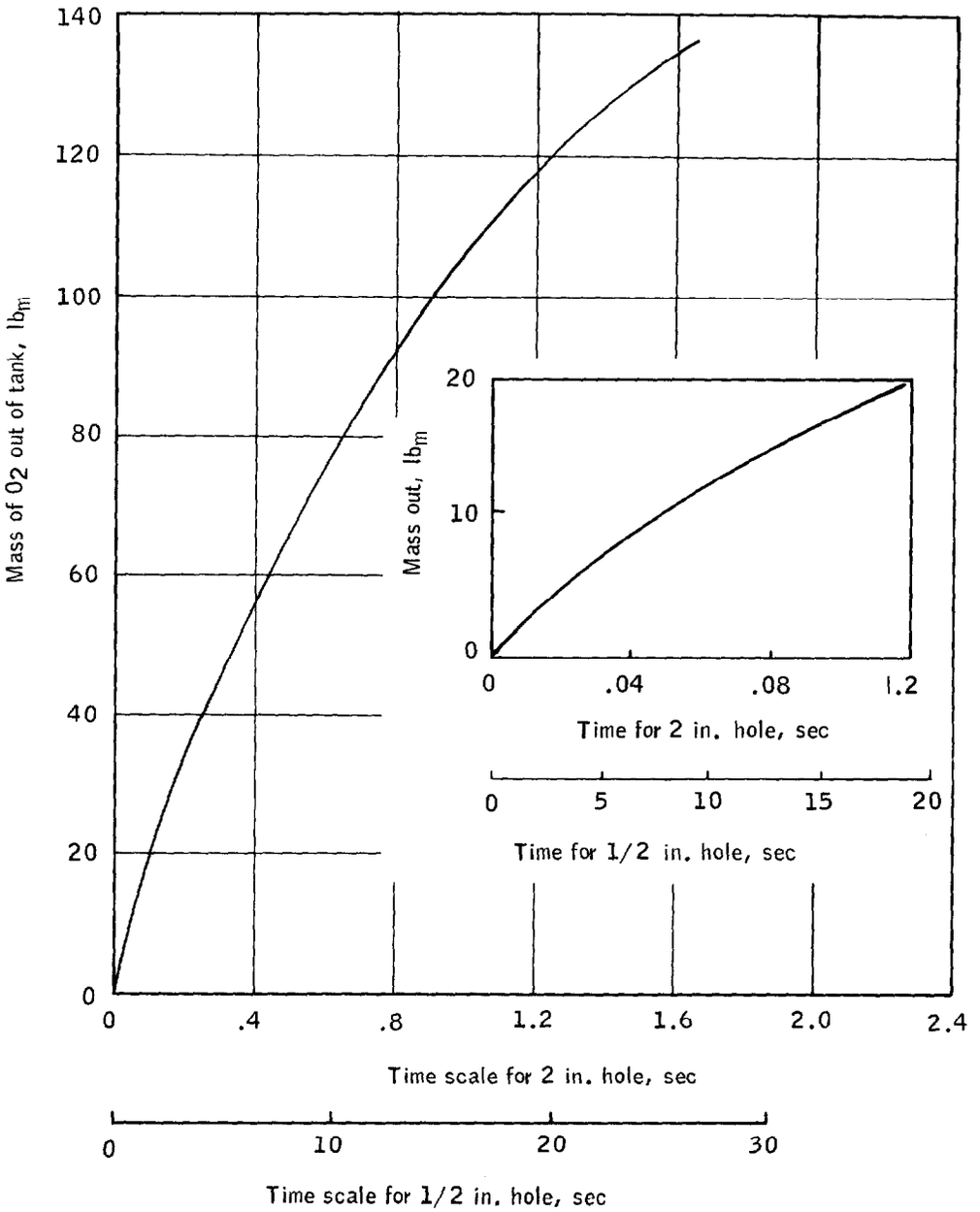

Figure F3.8-2.- Mass of oxygen expelled from tank against time.

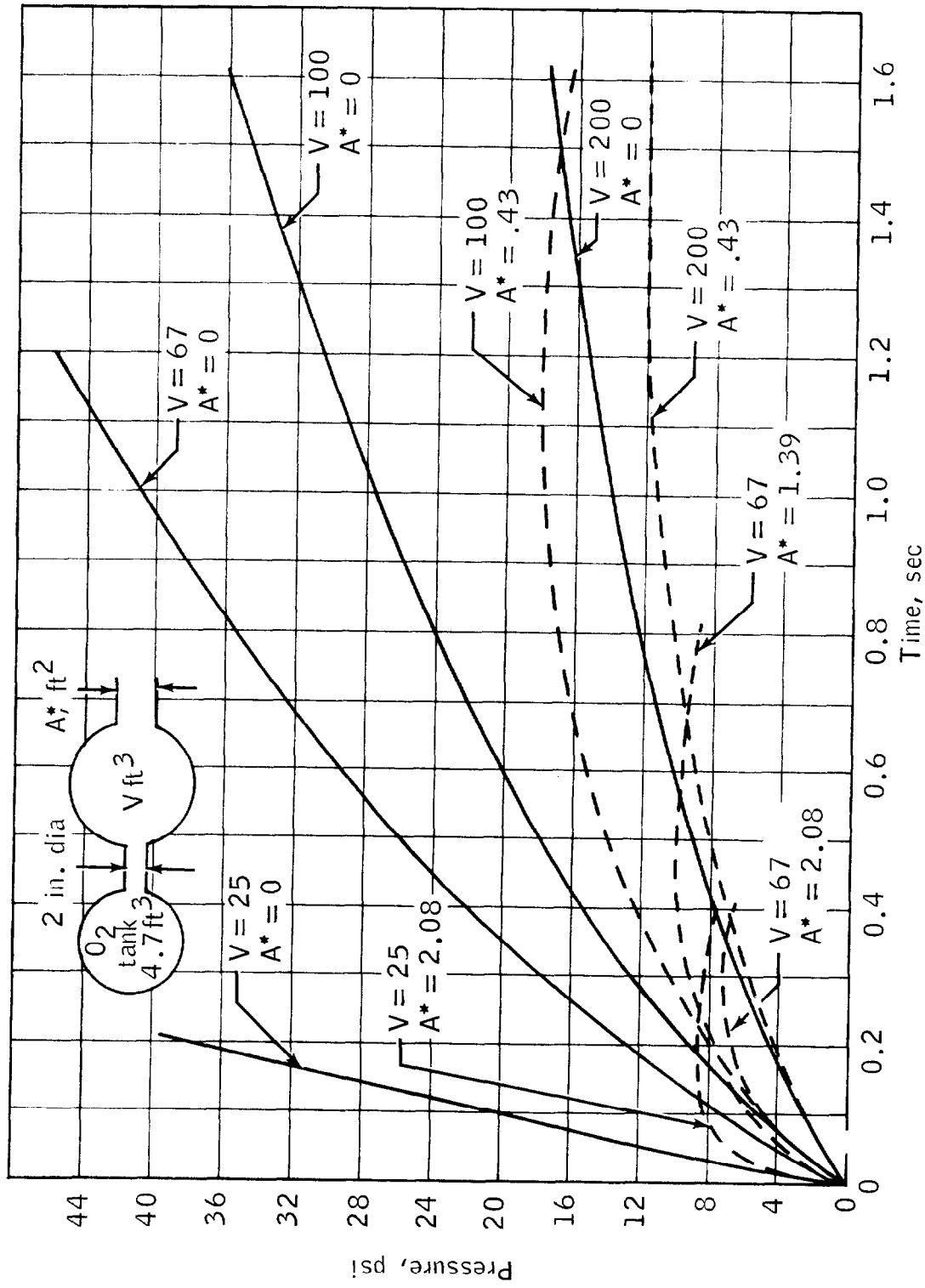

Figure F3.8-3.- Pressure rise against time.

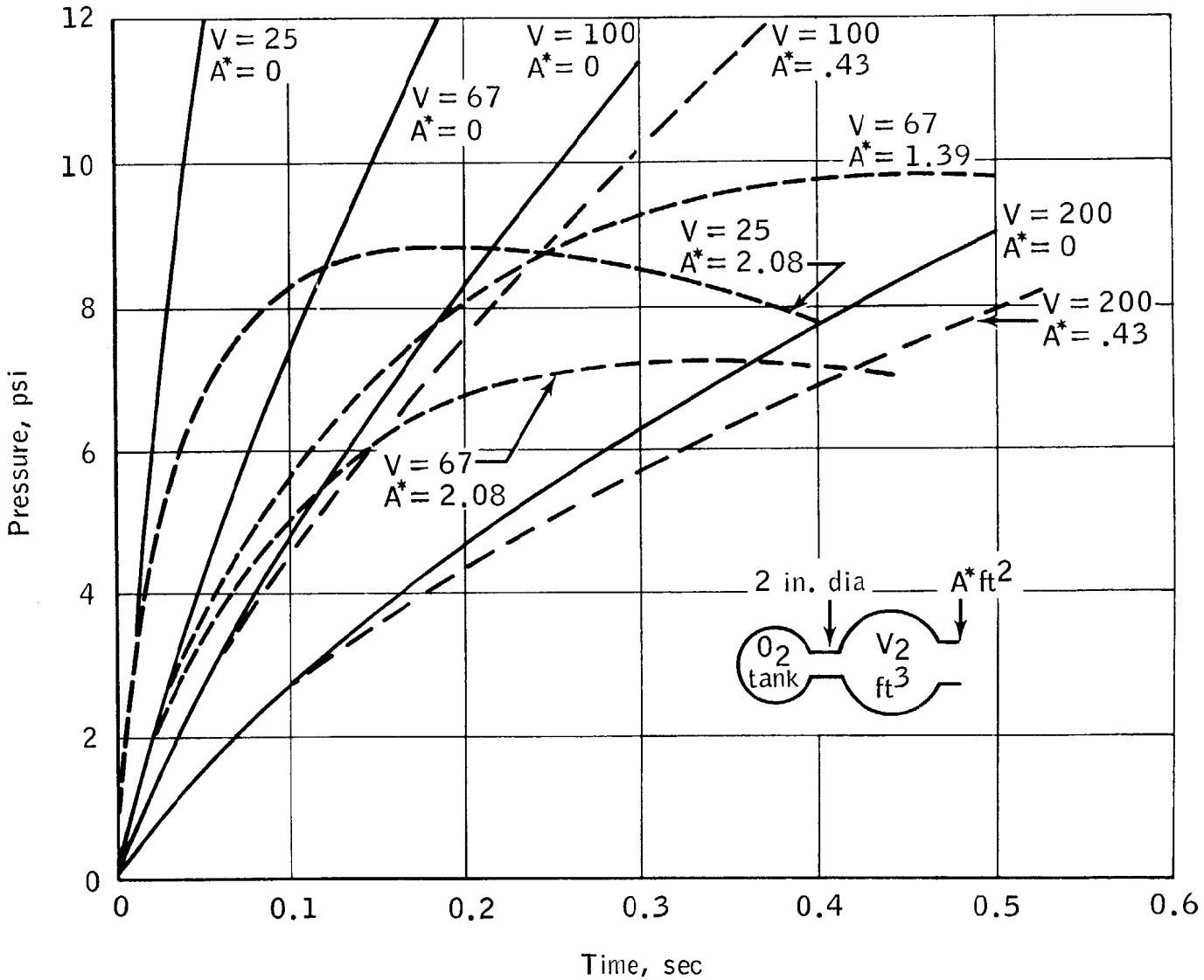

Figure F3.8-4.- Pressure rise against time (expanded scale).

The pressure of case 2, with V = 67 ft^3, rises less rapidly and consequently peaks at a later time (t = 0.32 sec) and a lower peak pressure (p $\approx$ 7.2 psi).

When the vent area for V = 67 ft^3 is decreased from 300 in^2 to 200 in^2 (case 3), the pressure rises more rapidly, peaks at a longer time (t $\approx$ 0.45 sec), and has a higher peak pressure (p $\approx$ 9.8 psia).

The large volume solutions with minimum vent areas (cases 4 and 5) have higher peak pressures (p $\approx$ 18 and 12 psia) occurring at much larger times (t = 1.1 and 1.5 sec).

Discussion and Conclusions

These "quasi-steady" two-volume, two-orifice, adiabatic calculations do not predict pressures in excess of 20 psia for a 2-inch diameter effective orifice in the oxygen tank. In fact, if the two larger volume simulations (cases 4 and 5) are excluded due to unrealistically low venting areas and/or the long time rise, then the maximum predicted pressure is below 10 psia. The smaller volumes representative of the oxygen shelf, or the oxygen shelf plus fuel cell shelf (which is fairly well intervented to the oxygen shelf) have shorter rise times which are more representative of the implied "time to panel failure" of Apollo 13. The effective venting area of these volumes is also more realistic.

On the basis of these approximate calculations, the following alternative possibilities might be considered:

1. The panel failure pressure is below 10 psi. Other experiments show this low failure pressure level to be unlikely.

2. The dynamic unsteady pressures exceed the computed quasi-steady pressures. A non-uniform pressure distribution with internal moving pressure waves is considered very probable with their importance being larger for the smaller times and volumes.

3. The oxygen tank orifice had an effective diameter greater than 2 inches. During the discharge of the first 9 pounds of oxygen, the orifice was choked with nearly saturated liquid oxygen and the coefficient was probably nearer 0.6 than 1. Thus an effective 2-inch diameter would require an even larger physical hole during this time.

4. The processes in the oxygen tank were not isentropic in a fixed volume. Either continued combustion inside the oxygen tank or the presence of a bubble of combustion products at the time of initial gas release could prevent the computed rapid decrease in mass flow with time (fig. F3.8-1) and therby increase the pressure rise rate and the peak pressure.

5. The processes in the external volume (V) are not adiabatic. Combustion of the Mylar insulation has been estimated to produce large pressures (several atmospheres) if the combustion process is rapid enough.

6. The oxygen processes are not in equilibrium. The possibility of super-satruation of the oxygen discharged into the bay and subsequent flashing to vapor might produce a strong pressure pulse.

PART F3.9

MYLAR-INSULATION COMBUSTION TEST

Objective

The purpose of this test was to determine the ignition properties and measure the rate of combustion of Mylar insulation in an initially evacuated simulated oxygen shelf space. The conditions of this test are achieved by ejection of oxygen from a 1000 psia/-190° F oxygen supply with ignition by pyrofuses placed on the Mylar blanket at several locations.

Apparatus

The basic dimensions and arrangement of the apparatus are shown in figure F3.9-1. An end view of the apparatus is shown in figure F3.9-2. Mylar blank material is placed on the bottom shelf. Oxygen is supplied through a regulator into a simulated tank dome volume. The dome contains a 2-inch diameter rupture disc which is designed to open at 80 psi. Pressures are measured during the course of combustion process. High-speed motion pictures are obtained through window ports in the chamber. The chamber volume and vent area simulate the oxygen tank shelf space.

Approach

Oxygen is supplied from a cryogenic source which is initially at 1000 psia/-190° F. Oxygen flows for a controlled time into the dome volume. The 2-inch disc ruptures at 80 psi. This exposes the initially evacuated chamber and its contents to a mixture of liquid and gaseous oxygen. A series of pyrofuses are then ignited in sequence. The data include high-speed motion pictures and pressure-time histories.

Results

A test in which oxygen was allowed to flow for 3 seconds from an initially 1000 psia/-190° F source resulted in complete combustion of a 14.5 ft^2 Mylar blanket sample. Five pyrofuses located at various locations on the Mylar blanket were sequentially activated at times ranging between 0.3 and 1.4 seconds after the disc ruptured. Examination of the chamber after this run showed that all of the Mylar blanket was consumed. The pressure rise rate with the addition of oxygen but before ignition was approximately 6 psi/sec. Ignition occurs when the pressure rises to

about 10 psi with subsequent combustion which causes a sharp increase in the pressure rise rate. The rate of pressure rise during the combustion process reaches approximately 42 psi/sec. The initial pressure rise rate of 6 psi/sec also corresponds to a measured rise rate obtained in an earlier test in which combustion did not occur. The pressure data are shown in figure F3.9-3. The conditions in the chamber before the test are shown in figure F3.9-4. Figure F3.9-5 shows the chamber just after the test.

Conclusion

The Mylar insulation blanket burns completely when ignited locally and exposed simultaneously to oxygen from a 1000 psi/-190° F source. The pressure rise rate increases from 6 psi/sec without combustion to about 42 psi/sec with the combustion of Mylar. A substantial increase in the pressure rise rate in the oxygen tank shelf space due to Mylar combustion might therefore be expected. From tests conducted elsewhere, it is further concluded that an ignition source is required to achieve Mylar/oxygen combustion.

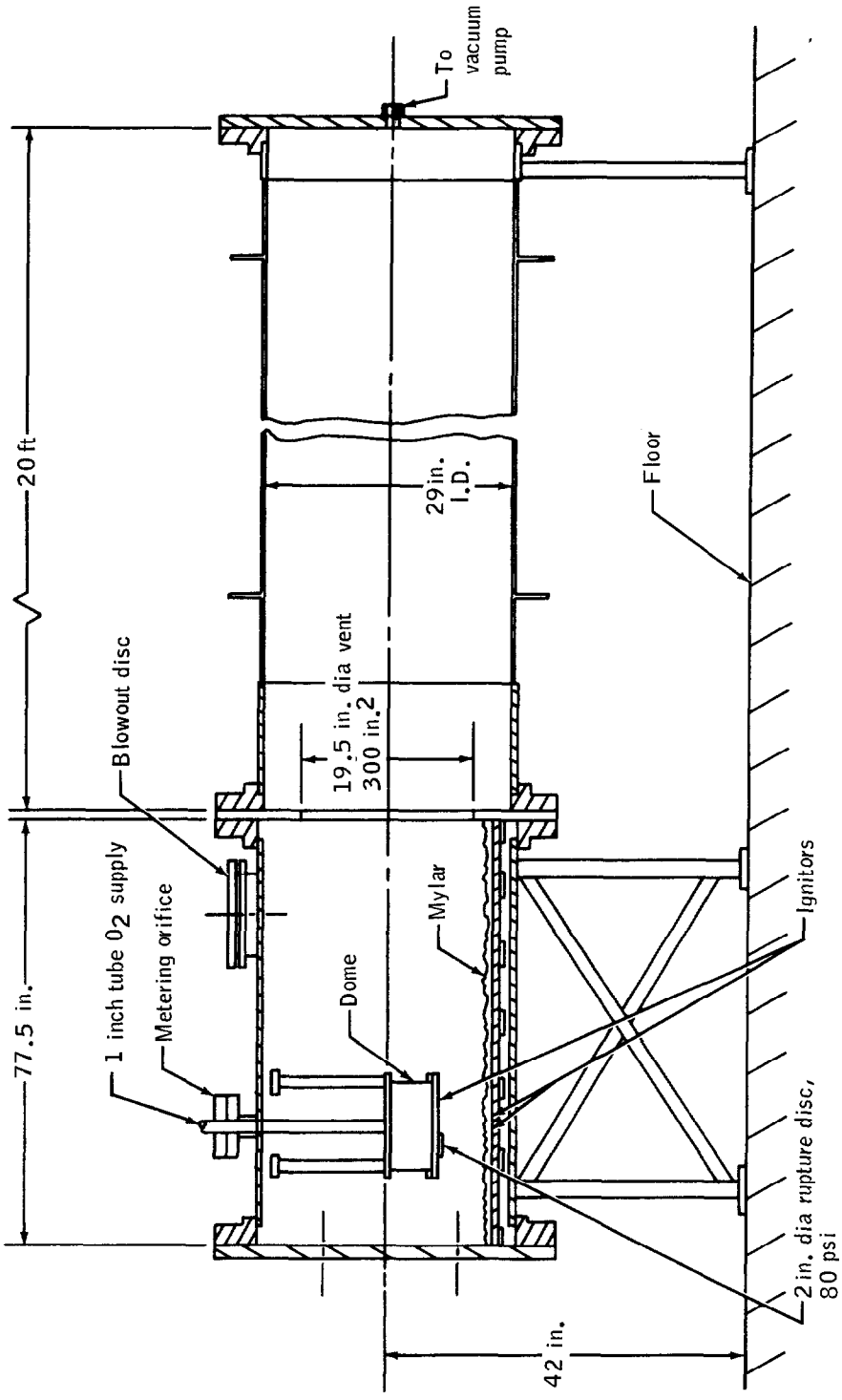

Figure F3.9-1.- Assembly of test fixture.

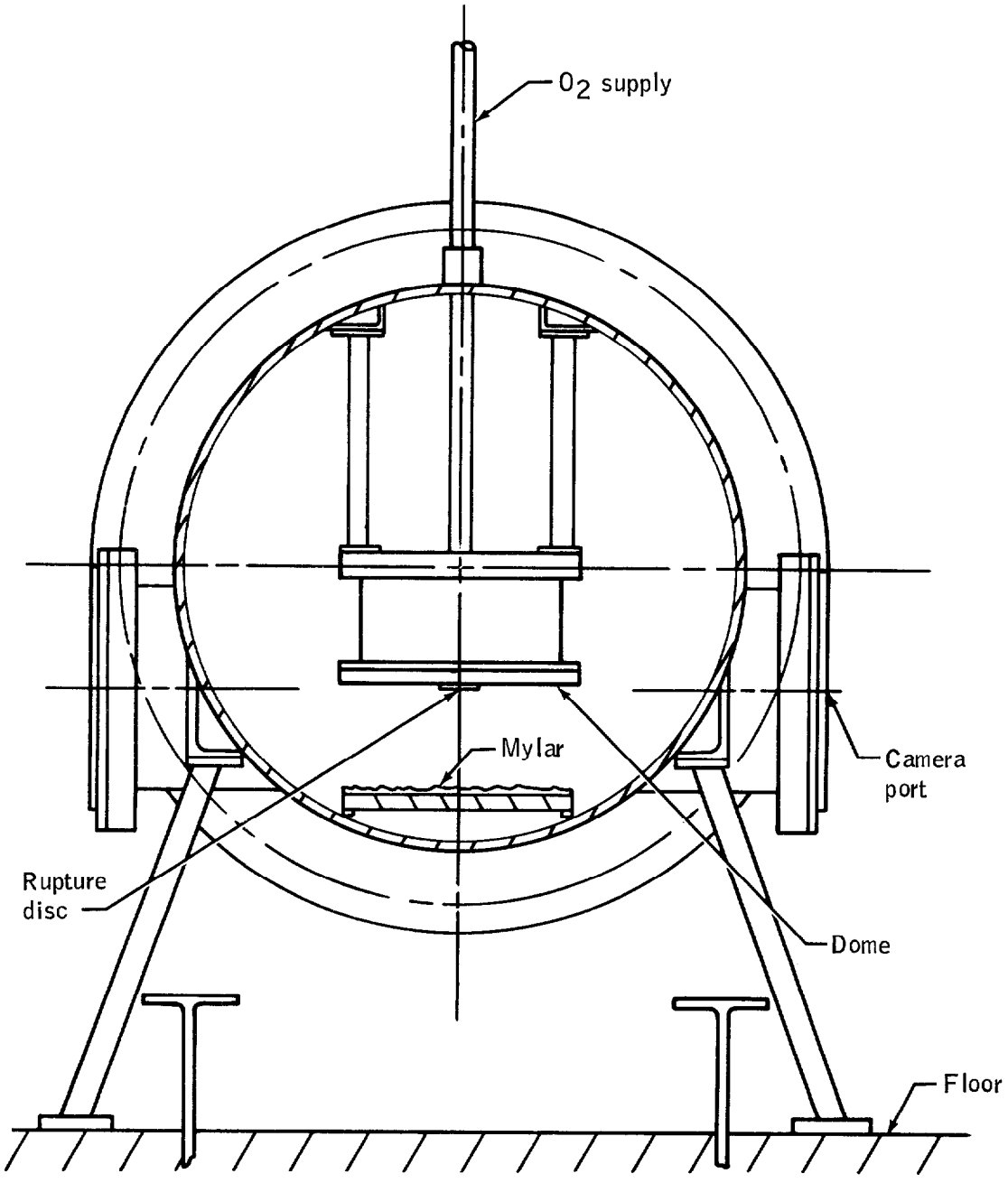

Figure F3.9-2.- Section through test fixture.

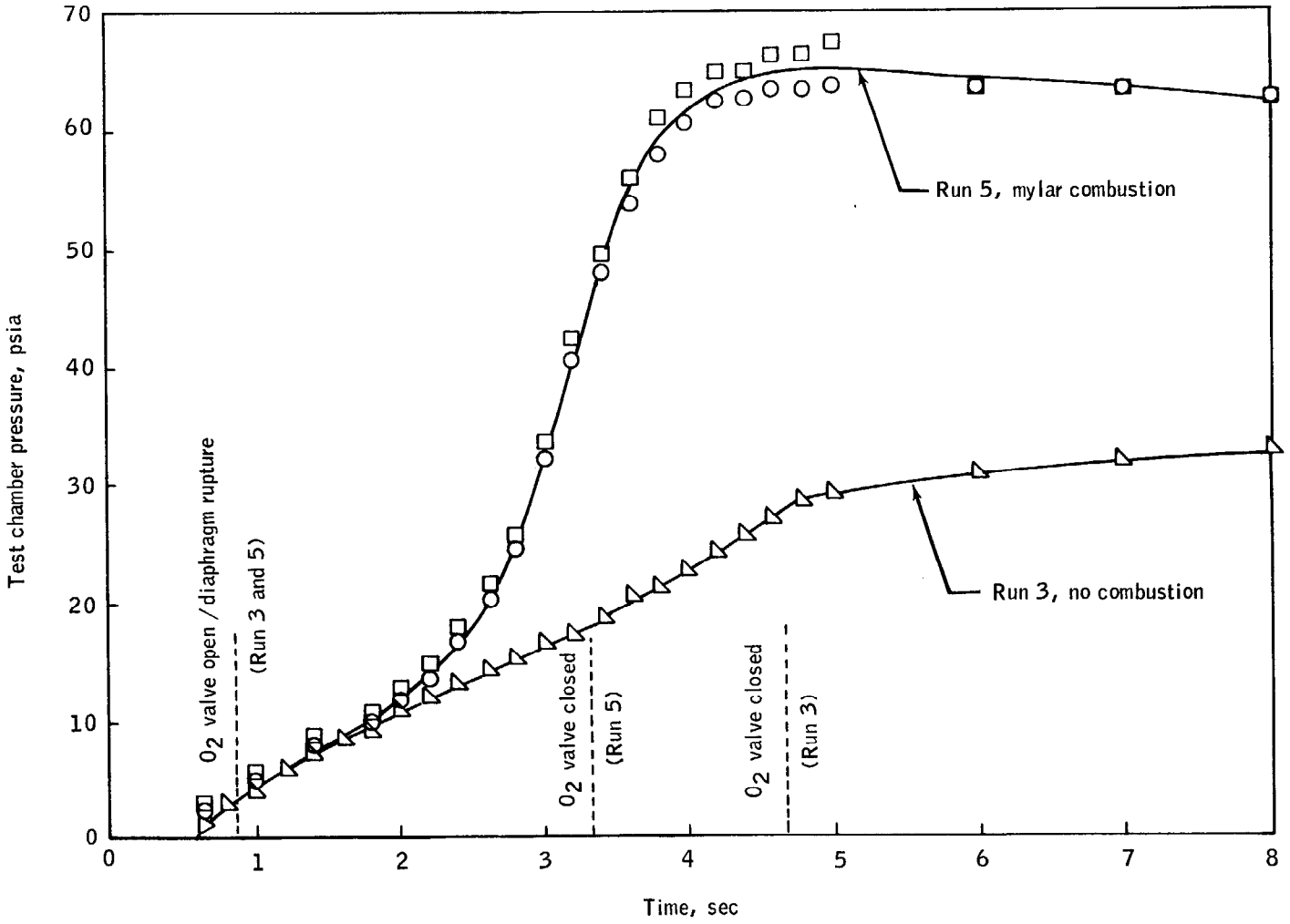

Figure F3.9-3.- Measured pressure histories for runs with and without Mylar combustion (initial oxygen tank temperature for Run 3 was -186° F and for Run 5 was -192° F).

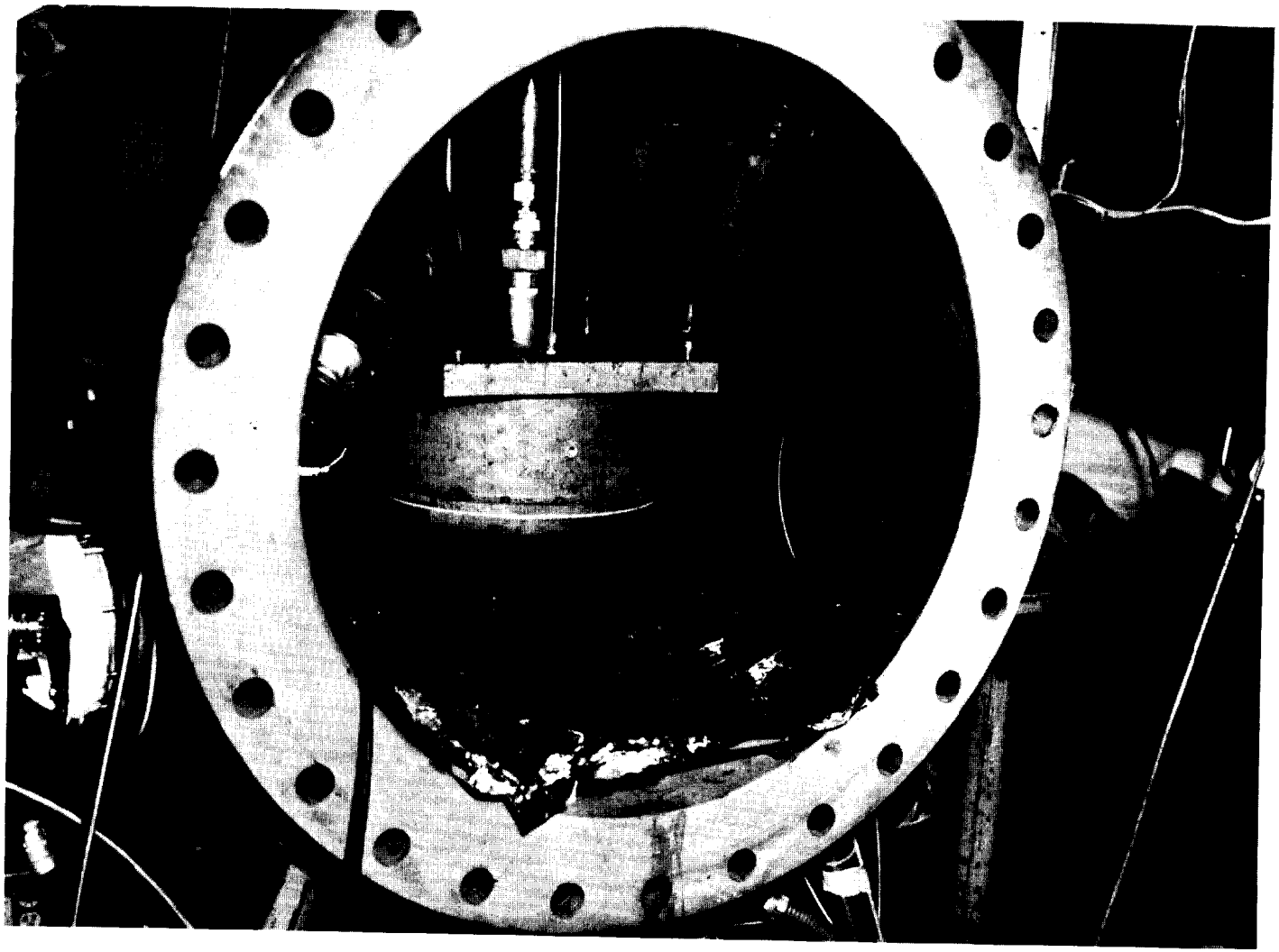

Figure F3.9-4.- View of chamber conditions before test.